Design of an injectable and bioerodible supramolecular hydrogel as a local nucleic acid delivery system

ACS APPLIED POLYMER MATERIALS

pubs.acs.org/acsapm
Article

Design of an Injectable and Bioerodible Supramolecular Hydrogel as a Local Nucleic Acid Delivery System

Paola Grillo Coppola,[#] Adrian Philipp Eckart Kromer,[#] Monica Boffito,[*] Benjamin Winkeljann, Gianluca Ciardelli,[*] and Olivia M. Merkel[*]

Cite This: *ACS Appl. Polym. Mater.* 2025, 7, 15856−15866

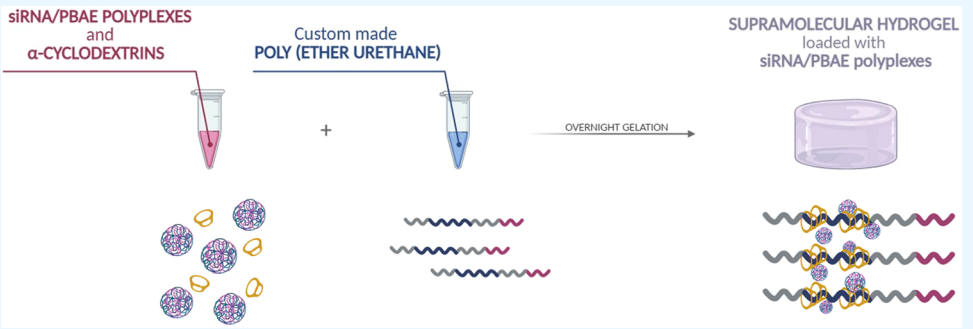

ABSTRACT: Although RNA therapeutics hold great promise for treating different diseases, their administration across physiological barriers remains challenging. This study explores a supramolecular (SM), bioerodible, and injectable hydrogel, composed of an *ad hoc* synthesized Poloxamer 407-based poly(ether urethane) (PEU) and α-cyclodextrins (α-CDs), as a carrier for localized delivery of poly(β-amino ester) (PBAE) and siRNA polyplexes. Polyplexes assembled within α-CDs showed higher sizes (150−300 nm) and positive charges (+20 to +30 mV) compared to those in HEPES buffer (<100 nm, −20 to +20 mV). SM hydrogels, prepared by mixing aqueous solutions of PEU and α-CDs at final concentrations of 0.9−1.4 and 10% w/v, respectively, preserved thixotropic and self-healing characteristics after polyplex embedding. Intact polyplexes were released from the hydrogel over 48 h and showed efficient gene knockdown in phagocytic cells. These findings underscore the potential of SM hydrogels as gene delivery vehicles, premised upon their injectability and favorable release profiles.

KEYWORDS: *polyplexes, supramolecular hydrogels, injectability, small interfering RNA, gene delivery*

1. INTRODUCTION

Injectable hydrogels are a class of materials with relevant shear-thinning behavior, allowing them to flow easily under shear stress, and self-healing capabilities, enabling them to recover their structure when the applied stress is relieved. Due to these features, injectable hydrogel formulations have found widespread application for controlled and prolonged release of various compounds, such as small molecules, proteins, and nucleic acids.[1,2] Indeed, payloads can be homogeneously included into the hydrogel while it is still in the liquid form, but, once in the gelified state, the typical shear-thinning and self-healing properties of these hydrogels enable smooth injection through needles without clogging and allow for recovery to their initial state once fully injected, with the advantage of being delivered to difficult to access sites without the need for surgery.[3,4] In case of RNA therapeutic release, hydrogels enable precise management of both spatial and temporal aspects, thus enhancing the therapeutic efficacy of RNA treatments. Several hydrogel designs have been utilized to achieve controlled RNA release, employing either passive or active mechanisms.[4−8] RNA molecules can be incorporated into hydrogels in two ways: either directly by including the naked RNA itself or by embedding RNA-containing nanocarriers within the hydrogel network. Phagocytic T-cells pose a special challenge in RNA delivery due to low uptake rates or moderate endolysosomal acidification and thereby low transfection efficiencies using classical nanocarriers.[9−11] However, there have been numerous strategies to overcome these obstacles such as the utilization of special polymers like VIPER (virus-inspired polymer for endosomal release) or targeting ligands.[12,13]

Utilizing RNA nanocarriers (e.g., liposomes/lipid nanoparticles, polymeric nanoparticles, inorganic nanomaterials)

Received: July 21, 2025
Revised: November 13, 2025
Accepted: November 16, 2025
Published: November 25, 2025

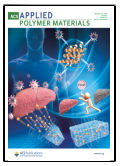

loaded within a hydrogel network offers distinct advantages over the direct delivery of naked RNA. This approach decreases the need for chemical modifications of both the RNA and hydrogel-forming materials while potentially enhancing the loading capacity, stability, and transfection efficiency. Furthermore, when RNAs are encapsulated in carriers, they are protected from nucleases, with a consequent increase in their longevity, and their endocytosis-mediated internalization followed by cargo release in the cytosol improves RNA uptake compared to extracellular release of naked RNA molecules. Among RNA-based drugs, small interfering RNAs (siRNAs) silence the expression of their target RNAs by exploiting the endogenous RNA interference (RNAi) pathway,[14,15] thus playing a crucial role in altering the expression or activity of its targeted molecules.[8]

Based on these premises, in this work, we report the incorporation of siRNA-based polyplexes into a custom-made injectable and bioerodible supramolecular hydrogel as a new nucleic acid delivery system for localized, sustained, and prolonged *in situ* release of RNA therapies through a passive mechanism.

Specifically, polyplexes were selected as nonviral siRNA nanocarriers overcoming the typical drawbacks of viral vectors (i.e., complex preparation, limited size of the foreign gene they can carry, potential for immunogenicity, and undesired mutations[16]). The majority of nonviral vectors is positively charged under physiological conditions (e.g., cationic polymers and cationic liposomes[17,18]) in order to interact with negatively charged nucleic acids.[19] These vectors enter target cells through endocytosis, and their preparation process is relatively straightforward.[20] In this category, poly(β-amino ester)s (PBAEs) are among the most extensively researched cationic polymers[21] due to their numerous advantages such as (i) the presence of positive charges for nucleic acid complexation, (ii) the presence of easily degradable linkages in the polymer backbone (i.e., hydrolyzable ester bonds) enhancing biodegradability and biocompatibility, and (iii) flexibility to customize the properties of the polymer through a combination of various monomers.[22,23] PBAEs have found successful application in numerous studies[22,2425] as transfection agents because they contain amino groups with pH-dependent positive charges that can engage in electrostatic interactions with the negative charges of nucleic acid phosphate groups,[25,26] thus forming a polyelectrolyte complex, commonly referred to as a polyplex.[27] In this work, a PBAE-based polyspermine with 75% oleyl amine side chain[28,29] (Figure S1) was complexed with siRNA to obtain polyplexes at different N/P ratios, further characterized regarding their hydrodynamic diameters, ζ-potentials, and siRNA encapsulation efficiency.

With regard to the hydrogel counterpart, supramolecular (SM) hydrogels relying on the combination of a synthetic poly(ethylene oxide) (PEO)-containing polymer with α-cyclodextrins (α-CDs) have been identified as potential polyplex carriers due to their relevant shear-thinning and self-healing properties and thus injectability.[30] Among commercially available PEO-based polymers, Poloxamer 407 (P407), also known as Pluronic F127, has been widely investigated for SM hydrogel design.[31] Although P407-based supramolecular gels exhibit relevant thixotropic and self-healing properties, making them easily injectable, being at the same time biocompatible, bioadhesive, and allowing for controlled drug release,[32] several drawbacks have also been reported in the literature, including phase separation, poor mechanical performances, and rapid dissolution.[33] In order to overcome these limitations and widen the tuning potential of P407-based SM hydrogel formulations, in the past years, we reported on the possibility of using P407 as macrodiol for the synthesis of high-molecular-weight poly(ether urethane)s and exploiting the resulting polymers as constituents of SM hydrogels upon mixing with α-CDs.[34−36] Within our group, supramolecular hydrogels have been employed as drug delivery systems for curcumin upon complexation with α-CDs[35] and lignin−cobalt nanoparticles for the treatment of bacterial infections in chronic wounds.[37] As a step forward, in this work, we report on the possibility of encapsulating siRNA-containing polyplexes into PEU-based SM gels. Specifically, PBAE-based polyplexes (PXs) containing siRNA were loaded into PEU-based SM hydrogels during their preparation by exploiting the possibility of preparing the polyplexes directly within the α-CD solution. Hydrogel gelation kinetics was then qualitatively evaluated through a tube inverting test, and mechanical and self-healing characteristics were assessed through rheological analysis, comparing PX-loaded hydrogels with the corresponding placebo formulations. The hydrogel's ability to release intact polyplexes over time was also assessed through dynamic light scattering, nanoparticle tracking analysis, and transmission electron microscopy. Finally, the polyplexes released from the hydrogels were tested on monocytes to investigate their gene silencing effects.

2. MATERIALS AND METHODS

2.1. Materials. 4-(2-Hydroxyethyl)-1-piperazine ethanesulfonic acid (HEPES), heparin sodium salt, dimethyl sulfoxide (DMSO), Triton-X 100, Atto 647, RPMI-1640 medium, heat-inactivated fetal bovine serum (FBS), penicillin/streptomycin solution, G418 disulfate salt solution, and Dulbecco's phosphate buffer saline (DPBS) were purchased from Sigma-Aldrich (Darmstadt, Germany). Double-stranded human glyceraldehyde 3-phosphate dehydrogenase (GAPDH) siRNA (5′-pGGUCGGAGUCAACGGAUUUGGUCgt, 3′-UUCCAGCCUCAGUUGCCUAAA-CCAGCA) and scrambled siRNA (5′-pCGUUAAUCGCGUAUAAUACGCGUat, 3′-CAG-CAAUUAGCGCAUAUUAUGCGCAUAp) were purchased from Integrated DNA Technologies (IDT, Coralville, Iowa, USA). Real-time PCR reagents and kits, 0.05% and 0.25% trypsin/ethylenediaminetetraacetic acid (Trypsin EDTA), Lipofectamine 2000 (LF), and Opti-MEM Serum Reduced Medium were purchased from Thermo Fisher Scientific (Schwerte, Germany). α-Cyclodextrins (α-CDs) were purchased from Glentham Life Sciences (Corsham, U.K.).

2.2. Polyplex Preparation and Characterization. A spermine-based amphiphilic poly(β-amino ester) (PBAE) containing 75% oleyl amine (OA) monomer was synthesized according to a previous protocol (Figure S1).[28] Hereafter, the polymer will be referred to with the acronym PBAE_75OA.

2.2.1. Polyplex (PXs) Preparation. The preparation of polyplexes took place either in sterile filtered 10 mM HEPES buffer (pH 5.4) or in 10 mM HEPES buffer (pH 5.4) containing α-CDs at 14% w/v concentration. To this aim, an α-CD solution at 14% w/v concentration in HEPES buffer (10 mM, pH 5.4) was first prepared and filtered through a 0.22 μm pore-sized syringe filter (Rotilabo-syringe filters, Carl Roth GmbH, Karlsruhe, Germany). In parallel, a DMSO stock solution containing PBAE_75OA at 25 mg/mL concentration was diluted at 1:10 volume ratio either in HEPES buffer or in α-CD containing HEPES buffer to obtain a PBAE_75OA final concentration of 2.5 mg/mL. For preparing the polyplexes, PBAE_75OA and siRNA solutions were then diluted to determined concentrations in a total volume of 100 μL of HEPES or α-CD containing HEPES buffer in order to obtain polyplexes at desired N/P

https://doi.org/10.1021/acsapm.5c02686
ACS Appl. Polym. Mater. 2025, 7, 15856−15866

Table 1. Volume of Each Solution Needed to Prepare 1 mL of Each Hydrogel Formulation and the Corresponding Sample Acronyms

hydrogel formulation	CHP407 3% w/v (μL)	CHP407 5% w/v (μL)	α-CD 14% w/v w/o PXs (μL)	α-CD 14% w/v with PXs (μL)
CHP407 0.9% + α-CD 10%	286		714	
CHP407 1.4% + α-CD 10%		286	714	
CHP407 0.9% + α-CD 10% + PX	286		357	357
CHP407 1.4% + α-CD 10% + PX		286	357	357

ratios (i.e., 5, 7, 10, and 15). The amount of PBAE_75OA needed for each N/P ratio was quantified through eq 1

$$m_{\text{PBAE\_75OA}} = n_{\text{siRNA}} \times 52 \times N/P \times M_{\text{protonable\_unit}} \quad (1)$$

where $m_{\text{PBAE\_75OA}}$ is the mass of the polymer in pg, n_{siRNA} is the amount of siRNA in pmol, 52 is the number of RNA's nucleotides, and $M_{\text{protonable\_unit}}$ is the molar mass of the protonable unit within the PBAE_75OA in pg/pmol. Finally, the two solutions of PBAE_75OA and siRNA were gently mixed at a volume ratio of 1:1 using a pipet (15−20 consecutive pipet mixing procedures) and allowed to incubate for 90 min at room temperature to allow PX formation. Hereafter, the prepared polyplexes will be referred to with the acronyms PX_HEPES and PX_HEPES + α-CD depending on the composition of the 10 mM HEPES buffer used for their assembly (i.e., the buffer as such or containing α-CDs at 14% w/v concentration). The hydrodynamic diameter and ζ-potential of both PX_HEPES and PX_HEPES + α-CD were tested using a Zetasizer Nano ZS (Malvern Instruments, Malvern, UK).

2.2.2. siRNA Encapsulation Efficiency. The amount of siRNA encapsulated within the polyplexes was estimated through a fluorescence-based quantification assay using the SYBR Gold Nucleic Acid Stain[38] (Life Technologies, Darmstadt, Germany). To estimate the encapsulation efficiency, 10 μL of each sample was incubated with 12 μL of RNase-free water for 1 h at 37 °C under shaking (300 rpm). After that, the samples were added in a 384-well black microplate (Greiner Bio-One, Frickenhausen, Germany) together with 3 μL of 4× SYBR Gold Nucleic Acid Gel Stain and incubated in the dark under shaking (300 rpm) at 37 °C for 10 min. As blank measurements, the same volumes of HEPES buffer or HEPES buffer containing α-CDs at 14% w/v were employed, while as 100% free siRNA reference, 10 μL of siRNA solution with the same concentration of the siRNA present in the formulations was used. Fluorescence was measured by means of a Spark microplate reader (Tecan, Männedorf, Switzerland) at 492 nm excitation and 537 nm emission wavelengths.

2.3. Hydrogel Preparation and Characterization. The poly(ether urethane) (PEU) used in this work for SM hydrogel preparation was synthesized according to a previous protocol (Figure S2)[34] starting from Poloxamer 407 (P407), 1,6-hexamethylene diisocyanate (HDI), and 1,4-cyclohexanedimethanol (CDM). The successful synthesis of a high-molecular-weight PEU (number-average molecular weight of 30 kDa and dispersity index of 1.8) was proved by size exclusion chromatography (SEC) (Agilent Technologies 1200 Series (Agilent Technologies, Inc., Santa Clara, CA, USA)), and attenuated total reflectance-Fourier transformed infrared (ATR-FTIR) spectroscopy (PerkinElmer Spectrum 100 (Waltham, MA, USA)). Based on its constituent blocks, the PEU used for hydrogel preparation will be identified with the acronym CHP407, where C, H, and P407 refer to CDM, HDI, and P407, respectively.

2.3.1. Preparation of SM Hydrogels Loaded with Polyplexes. CHP407 was solubilized at 3 and 5% w/v concentrations in HEPES buffer (pH 5.4) previously cooled to 4 °C and stored overnight at the same temperature to allow the polymer to fully dissolve. The polyplexes (N/P of 10) were prepared directly in HEPES buffer containing α-CDs at 14% w/v concentration as described in Section 2.2.1 and mixed with the CHP407 solutions by vortexing for 10 s. A schematic of the preparation protocol is illustrated in Figure S3. The ratio at which CHP407 and α-CDs solutions were mixed was defined to achieve a final α-CD concentration in the hydrogel of 10% w/v and a CHP407 concentration of 0.9 and 1.4% w/v, depending on the concentration of the starting CHP407 solution (i.e., 3 and 5% w/v, respectively). Based on nanoparticles tracking analysis (NTA) results (data not shown), the polyplexes were loaded at a final concentration of around $2{\cdot}10^{10}$ particles/ml of hydrogel, corresponding to a siRNA loading of *ca.* 0.107 nmol/mL of hydrogel (defined considering a mean siRNA encapsulation efficiency of 84%). The resulting formulations were incubated at room temperature overnight to ensure gelation. Control samples were also obtained by mixing CHP407 aqueous solutions with an α-CD solution prepared in HEPES buffer without polyplexes. Table 1 reports the volume of each solution needed to prepare 1 mL of each hydrogel formulation and the corresponding sample acronyms.

2.3.2. Evaluation of Hydrogel Gelation Time. Hydrogel gelation time was qualitatively assessed by performing the tube inverting test. To this aim, 500 μL of each SM hydrogel formulation was prepared in 2 mL Eppendorf tubes according to the protocol reported above. The samples were then incubated at 25 °C and their sol or gel states were monitored over time through vial inversion. The sol and gel states were defined by the "flow" or "no-flow" conditions over 30 s of vial inversion, respectively. During the first hour of incubation, the samples were monitored every 10 min, while for the remaining observation time, their sol or gel state was evaluated every 20 min.

2.3.3. Rheological Characterization. Rheological tests were performed on CHP407 1.4% + α-CD 10% and CHP407 1.4% + α-CD 10% + PX using a stress-controlled rheometer (MCR 100, Anton Paar GmbH, Graz, Austria) equipped with a temperature control unit and a 25 mm parallel plate geometry. Each sample (approximately 600 μL) was loaded on the lower plate of the instrument previously equilibrated at 25 °C, and the gap and normal force were set, respectively, at 0.6 mm and 0 N. Three tests were performed per sample at a temperature of 37 °C: (i) strain sweep test with strain range from 0.01 to 500% and angular frequency kept constant at 1 rad/s; (ii) frequency sweep test with angular frequency varying between 100 and 0.1 rad/s at 0.1% strain (within the linear viscoelastic region (LVE) defined through the strain sweep test); and (iii) strain test performed at 1 rad/s angular frequency through application of three cycles of low and high strain (0.1% applied for 120 s and 100% applied for 60 s) to better investigate the dynamic self-healing properties of the hydrogels. The last applied deformation was low strain in order to assess the residual mechanical properties.

2.3.4. Polyplex Release from the Hydrogel. The release kinetics of siRNA-loaded PXs from CHP407 1.4% + α-CD 10% + PX was characterized by preparing 500 μL of hydrogel in 2 mL Eppendorf tubes. CHP407 1.4% + α-CD 10% hydrogels were also prepared as negative control samples. Upon gel equilibration at 37 °C, 500 μL of HEPES buffer (pH 5.4) was added on top of the SM hydrogels (i.e., gel to buffer volume ratio set at 1:1). The samples were incubated (37 °C, 300 rpm) and centrifuged (12,000 rcf, 5 min, room temperature) at different time points (i.e., 2, 4, 8, 24, and 48 h). Thereafter, 500 μL of the supernatant was collected for siRNA quantification and replaced with the same volume of fresh buffer. All the supernatants collected were analyzed both at the DLS and at the microplate reader performing the SYBR Gold assay as described in Section 2.2.2. All the samples were stored at −20 °C and at the last time point they were thawed, and the released polyplexes were further analyzed at the NanoSight NS300 (Malvern Panalytical) with the NTA technique. Transmission electron microscopy (TEM, TECNAI G2 s-Twin microscope, Thermo Fisher Scientific, voltage 300 kV) was also exploited to observe the morphology of the polyplexes released from the hydrogel. To ensure accurate observation of the released

https://doi.org/10.1021/acsapm.5c02686
ACS Appl. Polym. Mater. 2025, 7, 15856−15866

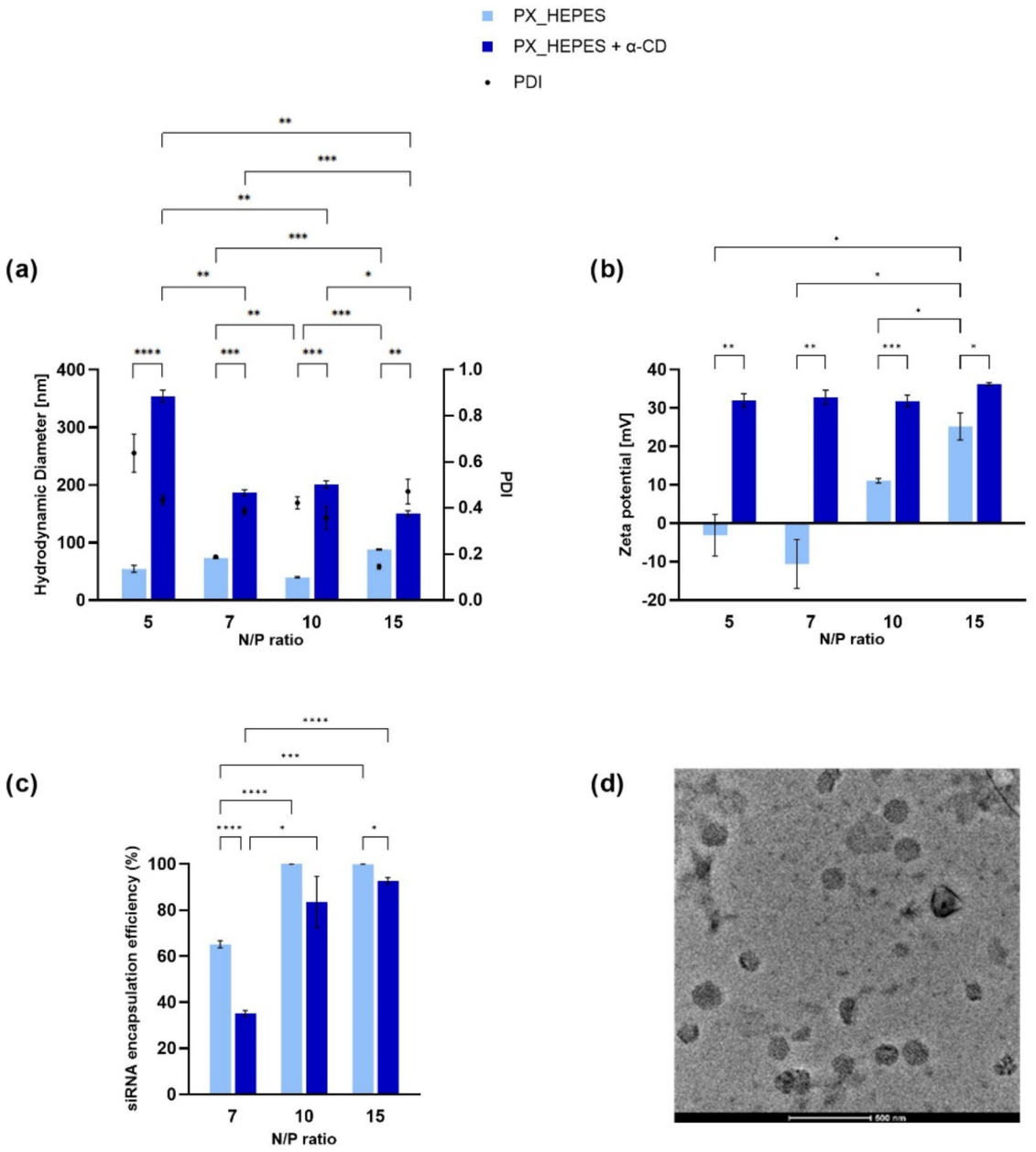

Figure 1. (a) Hydrodynamic diameter and PDI values of polyplexes prepared in 10 mM HEPES buffer pH 5.4 (light blue, PX_HEPES) and in 14% w/v α-CD solution in HEPES buffer (dark blue, PX_HEPES + α-CD). Hydrodynamic diameters (left y-axis, indicated as bars) and PDI (right y-axis, indicated as dots) at different N/P ratios: 5, 7, 10, and 15. (b) ζ-potential values of polyplexes prepared in 10 mM HEPES buffer pH 5.4 (light blue, PX_HEPES) and 14% w/v α-CD solution (dark blue, PX_HEPES+ α-CD). ζ-potential at different N/P ratios: 5, 7, 10, and 15. (c) siRNA encapsulation efficiency in PBAE polyplexes measured by the SYBR Gold assay at N/P ratios of 7, 10, and 15. Light blue bars: polyplexes prepared in HEPES buffer at pH 5.4 (PX_HEPES). Dark blue bars: polyplexes prepared in α-CD solution at 14% w/v concentration in HEPES buffer (PX_HEPES + α-CD). Data points indicate mean ± SD, n = 3. The statistical analysis reported on the graph is referred exclusively to the hydrodynamic diameter, ζ-potential, and encapsulation efficiency values. (d) Representative TEM image of as prepared polyplexes at an N/P ratio of 10. TEM imaging was performed on polyplexes in HEPES buffer 90 min after their assembly. Scale bar: 500 nm.

polyplexes, a 250 μL hydrogel sample was prepared by concentrating the polyplex solution up to 6 times. Subsequently, the hydrogel was incubated at 37 °C for 48 h under shaking conditions (300 rpm) in contact with 50 μL of HEPES buffer. For sample preparation, the supernatant was placed on a carbon-coated copper grid, and a staining solution (2% w/v phosphotungstic acid, Sigma-Aldrich) was placed on the top.

2.4. *In Vitro* Cell Testing. The MH-S cell line, which is an alveolar macrophage murine cell line, was cultured in RPMI-1640 medium supplemented with 10% FBS, 1% penicillin/streptomycin (v/v), and 0.05 mM β-mercaptoethanol. The cells were passaged every 2−3 days employing 0.25% Trypsin EDTA.

The THP-1 cell line, which is a cell line isolated from peripheral blood from an acute monocytic leukemia patient, was cultured in RPMI-1640 medium supplemented with 10% FBS, 1% penicillin/streptomycin (v/v), and 0.05 mM β-mercaptoethanol. The cells were passaged every 4 days. All the cell lines were cultured in 75 cm^2 culture flasks (Greiner Bio-One, Frickenhausen, Germany) and maintained in a humidified atmosphere (5% CO_2, 37 °C).

2.4.1. Polyplex Cellular Uptake. The ability of the polyplexes to enter the cells was verified through an uptake test run on the MH-S

https://doi.org/10.1021/acsapm.5c02686
ACS Appl. Polym. Mater. 2025, 7, 15856−15866

cell line. Macrophages were seeded in a 24-well plate (50,000 cells/ml in 500 μL of medium) and incubated for 24 h (5% CO_2, 37 °C). Thereafter, the cells were treated with 100 μL of the following solutions: (i) polyplexes freshly prepared in HEPES buffer (pH 5.4) (PX_HEPES), (ii) polyplexes prepared in α-CD (14% w/v) containing HEPES buffer (pH 5.4) (PX_HEPES + α-CD), (iii) polyplexes released from the hydrogel (CHP407 1.4% + α-CD 10% + PX) after 24 h of incubation at 37 °C (RELEASED_PX_24h), and (iv) polyplexes released from the hydrogel (CHP407 1.4% + α-CD 10% + PX) after 48 h of incubation at 37 °C (RELEASED_PX_48h). Lipofectamine 2000 lipoplexes were used as a positive control. The negative control was represented by untreated cells. PX_HEPES and PX_HEPES + α-CD were prepared as explained in Section 2.2.1 with 50 pmol/well of siNC labeled with 10% Atto 647 siRNA. For what concerns the polyplexes released from the hydrogel, they were concentrated up to 6 times their initial concentration before embedding them into the hydrogels, to obtain a release medium containing PXs at the same concentration as in the control samples. In more detail, both the PBAE and the siRNA concentrations were increased by 6-fold during PX preparation to obtain more polyplexes within the same volume. The hydrogels (500 μL, CHP407 1.4% + α-CD 10% + PX) were incubated in 2 mL Eppendorf tubes with 350 μL of HEPES buffer (37 °C, 300 rpm) for 24 and 48 h, and the collected supernatant was used to treat the cells. After 24 h of incubation, the cells were collected and analyzed by means of a flow cytometer using 638 nm excitation and a 670/14 nm bandpass emission filter set. Median fluorescence intensity (MFI) was obtained by analyzing at least 10,000 viable cells.

2.4.2. Polyplex-Mediated Gene Silencing. The ability of the polyplexes to silence gene expression was assessed by conducting qPCR tests. THP-1 cells were seeded in a 24-well plate (50,000 cells/ml in 500 μL of medium) and incubated for 24 h (5% CO_2, 37 °C). Thereafter, the cells were treated with 100 μL of the following solutions: polyplexes freshly prepared with siGADPH in (i) HEPES buffer (PX_HEPES) and in (ii) α-CD (14% w/v) containing HEPES buffer (pH 5.4) (PX_HEPES + α-CD), (iii) polyplexes released from the hydrogel (CHP407 1.4% + α-CD 10% + PX) after 24 h of incubation at 37 °C (RELEASED_PX_24h), and (iv) polyplexes released from the hydrogel (CHP407 1.4% + α-CD 10% + PX) after 48 h of incubation at 37 °C (RELEASED_PX_48h). Lipofectamine 2000 lipoplexes were used as positive control. The negative control was represented by untreated cells. Fresh polyplexes and hydrogel release media were prepared as described above (Section 2.4.1). After 48 h of incubation, the cells were collected and RNA extraction was carried out using a PureLink RNA Mini Kit (Thermo Fisher Scientific), following the manufacturer's protocol. Subsequently, complementary DNA (cDNA) was synthesized using a high-capacity cDNA reverse transcription kit (Thermo Fisher Scientific) and subjected to 40 cycles of qPCR amplification. For this purpose, SYBR Green qPCR kit was utilized (Thermo Fisher Scientific). The expression of the GADPH gene's mRNA was normalized to the expression of β-actin. Data were elaborated according to the following equations of normalization to endogenous expression control (eq 2), normalization to the reference sample (eq 3), and to finally obtain the fold change calculation (eq 4)

$$\Delta C_q = C_q[\text{Target}] - C_q[\text{Endogenouscontrol}] \quad (2)$$

$$\Delta\Delta C_q = \Delta C_q[\text{Sample}] - \Delta C_q[\text{Reference}] \quad (3)$$

$$RQ = 2 - \Delta\Delta C_q \quad (4)$$

where C_q refers to the cycle number at which the fluorescence signal generated by the amplification of the target DNA molecule crosses a specific threshold level. C_q[Target] is the C_q value related to the GADPH gene, while C_q[Endogenous control] is the C_q value related to the β-actin gene. Finally, the value of ΔC_q[Reference] was determined using a reference sample composed of water.

2.5. Statistical Analysis. Results are presented as the mean ± standard deviation. The notation "$n = 3$" indicates an experimental triplicate; i.e., it specifies that the experiment has been repeated 3 times with technical replicates to obtain more reliable results.

To assess the data, a two-way ANOVA analysis was conducted on data regarding polyplex characterization, while one-way ANOVA analysis was performed on data related to *in vitro* cell testing. Statistical analysis was carried out employing GraphPad Prism 9 software (La Jolla, CA, USA). The notation * refers to $p < 0.05$, ** to $p < 0.01$, *** to $p < 0.001$, and **** to $p < 0.0001$.

3. RESULTS AND DISCUSSION

3.1. Polyplex Characterization. *3.1.1. Hydrodynamic Diameter and ζ-Potential.* The hydrodynamic diameter and PDI values of polyplexes prepared in HEPES buffer as such and added with α-CDs (PX_HEPES and PX_HEPES + α-CD, respectively) are shown in Figure 1a. The hydrodynamic diameter of the polyplexes prepared in pure HEPES buffer was below 80 nm (as confirmed by TEM imaging in Figure 1d) with slight variations depending on the N/P ratio. On the other hand, the polyplexes prepared in HEPES + α-CD solution showed a hydrodynamic diameter below 200 nm except for the N/P value of 5 where the PX size was approximately 380 nm. This high variation was most likely due to the presence of α-CDs that, at a low N/P ratio, destabilized the PX formulation colloidally. The PDI of the polyplexes prepared in HEPES buffer was below 0.2, indicating a narrow size distribution. On the contrary, the PDI values of the polyplexes prepared in HEPES + α-CD solution were between 0.3 and 0.5. This increase may be due to the occurrence of α-CDs aggregation phenomena in an acidic environment (pH 5.4), resulting in the detection of bigger and more dispersed particles by DLS analysis.[39] Overall, the conducted DLS measurements highlighted that the prepared particles exhibited favorable characteristics for subsequent uptake and gene knockdown,[28] in particular for higher N/P ratios (i.e., 10 and 15).

With regard to the ζ-potential (Figure 1b), an increasing trend starting from negative values (approximately −10 mV) to positive values (+25 mV) was observed as the N/P ratios increased in the case of polyplexes prepared in HEPES buffer. On the contrary, it remained constant at +30 mV in the case of polyplexes prepared in HEPES + α-CD solution, irrespective of the tested N/P ratios. This outcome can be explained by referring to the α-CD pK_a value that is between 12.1 and 13.5; therefore, when in an acidic solution, α-CDs are protonated, thus enhancing the superficial charge.[39]

3.1.2. siRNA Encapsulation Efficiency. Since positive ζ-potential values, and lower PDI and hydrodynamic diameters are favorable for a successful cellular uptake,[40] the N/P ratio of 5 was excluded from the encapsulation efficiency analysis. Hence, the siRNA encapsulation efficiency was investigated on polyplexes prepared at N/P ratios of 7, 10, and 15. In detail, the SYBR Gold stain was used to quantify the amount of free siRNA (i.e., not encapsulated siRNA remaining in solution after polyplex assembly) thanks to its ability to emit fluorescence when intercalating with nucleic acids. The assay was performed both on the polyplexes prepared in HEPES and HEPES + α-CD, and the results are summarized in Figure 1c. The encapsulation efficiency values were comprised between 70 and 100% for the polyplexes prepared in HEPES, consistent with previous studies,[41] while they were lower for the polyplexes prepared in HEPES + α-CD. Therefore, it is reasonable to conclude that α-CDs slightly affected the encapsulation efficiency, with a more remarkable effect at the

https://doi.org/10.1021/acsapm.5c02686
ACS Appl. Polym. Mater. 2025, 7, 15856−15866

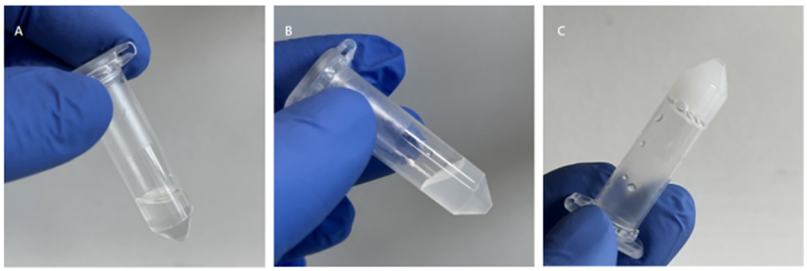

Figure 2. Progressive sol-to-gel transition of the hydrogel solution with the acronym CHP407 1.4% + α-CD 10% + PX. Appearance of the hydrogel solution (A) immediately after preparation and (B) after 1 h incubation. (C) Appearance of the assembled gel after the completion of the gelation process. The sample was incubated at room temperature (25 °C) and inverted at predefined time points to assess gelation.

N/P of 7. This observation could be explained considering that cyclodextrins can interact with the siRNA, being negatively charged, thus not permitting an unhindered assembly of the polyplexes.[42] Additionally, the hydrophobic part of the PBAE could form inclusion complexes with cyclodextrins, or α-CDs could act as hosts for siRNA molecules.[43] Although the encapsulation efficiency decreased in the presence of α-CDs, it could still be considered reasonable for the N/P ratios of 10 (no significant differences between PX_HEPES and PX_HEPES + α-CD) and 15 (significantly higher encapsulation for PX_HEPES *vs.* PX_HEPES + α-CD, $p < 0.05$). Nevertheless, the N/P ratio of 10 was selected for all subsequent experiments, since it allowed for a reduction in the amount of material (both PBAE and siRNA) employed for PX preparation compared to the N/P ratio of 15, with no relevant variation in the physicochemical characteristics of the resulting PXs (200 nm *vs.* 150 nm ($p < 0.05$), + 32 *vs.* +36 mV (no significant difference), encapsulation efficiency of 84 *vs.* 93% (no significant difference)).

3.2. Supramolecular (SM) Hydrogel Characterization.

3.2.1. Gelation Kinetics. The tube inverting test was initially conducted to macroscopically and qualitatively assess potential changes in the SM hydrogel gelation potential due to polyplex encapsulation. Based on a previous study,[34] the formulations were prepared with and without polyplexes (prepared at the N/P ratio of 10) starting from CHP407 PEU (0.9 and 1.4% w/v concentration) and α-CDs (10% w/v concentration) stock solutions. The prepared samples were identified with the acronyms reported in Table 1.

The gelation process is shown in Figure 2 and schematized in Figure S4: the opacity of the formulation increased as the supramolecular interactions occurred to reach a final white gel that did not show any flow on the walls of the vial upon inversion.

In general, the inclusion of polyplexes within the hydrogel strongly affected gelation potential and time of the developed formulations (Table 2). Indeed, in the absence of PXs, both CHP407 0.9% + α-CD 10% and CHP407 1.4% + α-CD 10% underwent gelation at room temperature in a time frame ranging between 6 and 12 h. Conversely, upon PXs addition, gelation was observed only for the formulation with the acronym CHP407 1.4% + α-CD 10% + PX upon overnight incubation at room temperature.

Table 2. Gelation Time at Room Temperature Qualitatively Estimated by Means of the Tube Inverting Test

formulation	gelation time
CHP407 0.9% + α-CD 10%	overnight
CHP407 0.9% + α-CD 10% + PX	no gelation
CHP407 1.4% + α-CD 10%	6 h
CHP407 1.4% + α-CD 10% + PX	overnight

3.2.2. Rheological Characterization. A series of rheological tests (i.e., frequency sweep test, strain sweep test, and self-healing strain test) was conducted on the formulations with acronyms CHP407 1.4% + α-CD 10% and CHP407 1.4% + α-CD 10% + PX, to better investigate the influence of the presence of PXs on the gel network features.[35] First of all, strain sweep tests were carried out to assess the linear viscoelastic region (LVE), which was measured to extend (γ_L) up to 3% for both CHP407 1.4% + α-CD 10% and CHP407 1.4% + α-CD 10% + PX. Both formulations (PXs loaded and unloaded) exhibited network complete disruption at strains around 30%, identified as the crossing point between the storage modulus (G') and the loss modulus (G''), as depicted in Figure 3a. This result confirmed that the encapsulation of polyplexes within the hydrogel formulation had a low impact on its thixotropic properties, the flow point being achieved at approximately the same strain value (γ_F of 30% *vs.* 32% for CHP407 1.4% + α-CD 10% and CHP407 1.4% + α-CD 10% + PX, respectively). Nevertheless, PX embedding provided the resulting gels with lower storage and loss moduli values within the LVE (Table 3), suggesting that they act as defects within the formulation, influencing gel network assembly and leading to less packed gels. This difference was further confirmed by frequency sweep tests that were conducted at 37 °C and 0.1% to ensure gel network preservation during the test. Indeed, G' values of 1610 and 1210 Pa were measured at 1 rad/s for CHP407 1.4% + α-CD 10% and CHP407 1.4% + α-CD 10% + PX, respectively. Nevertheless, the gel-like behavior of both the formulations was confirmed by registering the G' and G'' trends as a function of angular frequency (Figure 3b): G' constantly surpassed G'', and both the moduli were almost independent over angular frequency as typical of developed gels. Finally, the hydrogel capacity to regain its original properties after experiencing significant deformations was assessed through self-healing strain tests. As depicted in Figure 3c and summarized in Table 3, after three cycles of low and high strain, the G' value decreased by 7 and 14% for CHP407 1.4% + α-CD 10% and CHP407 1.4% + α-CD 10% + PX, respectively. These results evidenced that the self-healing properties of the system were influenced by the incorporation of polyplexes that slightly hindered gel network recovery upon rupture.

3.2.3. Polyplex Release from the Hydrogel. In order to gain a comprehensive understanding of PXs release dynamics from the developed formulations, multiple investigations were conducted on the samples collected in the polyplex release

https://doi.org/10.1021/acsapm.5c02686
ACS Appl. Polym. Mater. 2025, 7, 15856−15866

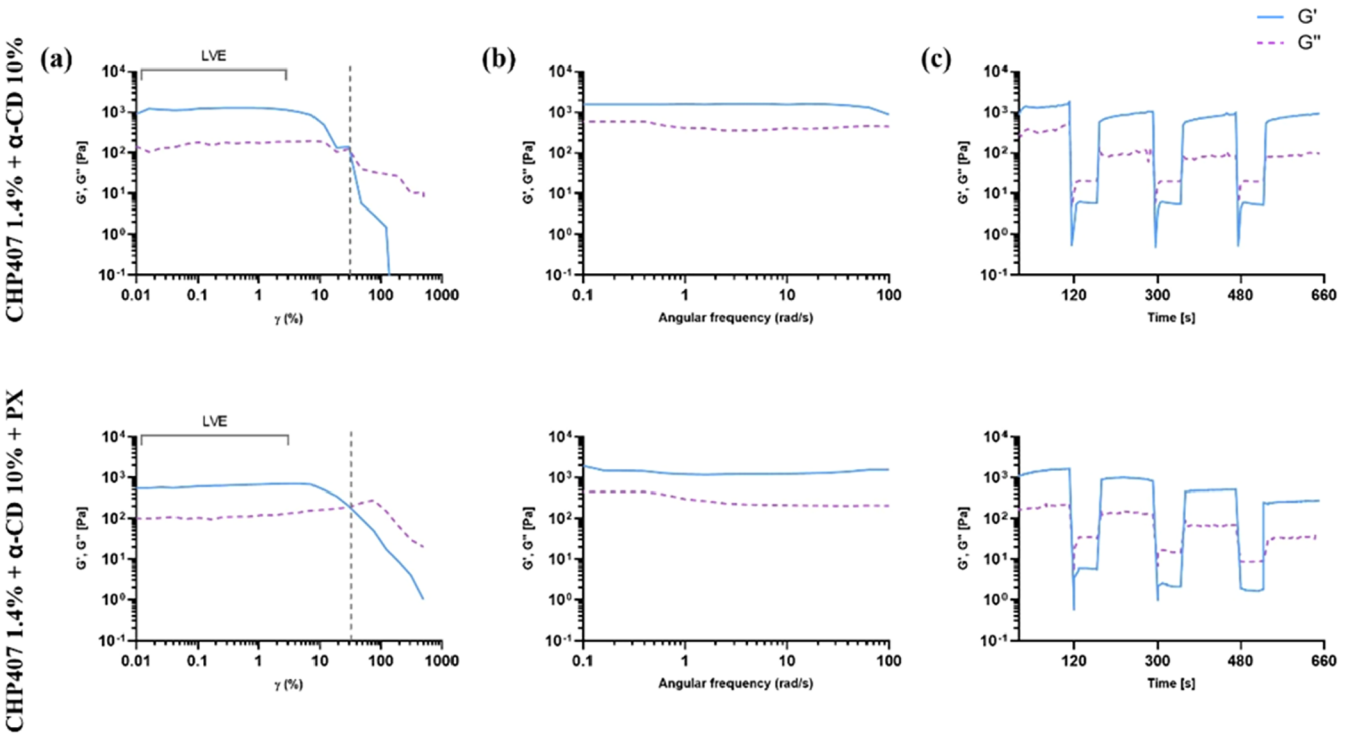

Figure 3. Rheological characterization of CHP407 1.4% + α-CD 10% and CHP407 1.4% + α-CD 10% + PX formulations. (a) strain sweep test at 37 °C, 1 rad/s, and within the strain range between 0.01 and 500%, (b) frequency sweep test at 37 °C, 0.1% strain and within the angular frequency range from 100 to 0.1 rad/s, and (c) self-healing strain test at 37 °C and 1 rad/s angular frequency through application of three cycles of low and high strain (0.1% applied for 120 s and 100% applied for 60 s), followed by low strain application for 120 s. G' (blue) and G'' (purple) are plotted as a function of strain (γ) for the strain sweep test, of angular frequency for the frequency sweep test, and time for the self-healing strain test.

Table 3. Summary of the Rheological Characteristics of CHP407 1.4% + α-CD 10% and CHP407 1.4% + α-CD 10% + PX Hydrogels Extracted from the Strain Sweep Test, Frequency Sweep Test, and Self-Healing (SH) Strain Test[a]

	strain sweep test				frequency sweep test	SH strain test
	γ_L (%)	γ_F (%)	G'_{LVE} (Pa)	G''_{LVE} (Pa)	$G'_{1\ rad/s}$ (Pa)	G' recovery (%)
CHP407 1.4% + α-CD 10%	3	30	1250	155	1610	93
CHP407 1.4% + α-CD 10% + PX	3	32	637	110	1210	86

[a] γ_L represents the strain value at the limit of the LVE region, γ_F represents the strain value at the flow point identified by the crossover between G' and G'' in strain sweep tests, G'_{LVE} and G''_{LVE} are the values of G' and G'' measured within the LVE, $G'_{1\ rad/s}$ is the G' value measured at 1 rad/s in the frequency sweep test, G' recovery is the percentage recovery in the G' value defined by comparing the G' values measured during the first and the last recovery phase in the strain test.

tests. DLS measurements were first conducted on the collected release media at different time points (i.e., 2, 4, 24, and 48 h of incubation), and the results are summarized in Figure 4a. However, the interpretation of the measured hydrodynamic diameter data was challenging due to prior studies indicating that the destabilization/dissolution of SM hydrogels in aqueous media is associated with the release of various components such as free α-CDs and polymeric chains/micelles.[35] Consequently, the DLS device detected all these components alongside polyplexes, impacting the final results in terms of both the size and PDI. After 2 h of incubation, the DLS measurement showed the release of large and highly dispersed particles with a mean dimension of around 250 nm and PDI of *ca.* 0.6. This supernatant probably included the immediately released erosion products from the hydrogel, containing PXs. Then, the dimension and PDI of the released particulate both decreased, showing values suggesting that some intact PXs were probably released with a size that increased over time, reaching a maximum value of *ca.* 180 nm. Interestingly, the PDI value of the released particles was lower than the measured value for freshly prepared PXs in HEPES + α-CD (i.e., 0.2 *vs. ca.* 0.4), suggesting that the dilution of α-CD upon release decreased interactions with PXs and their tendency to form aggregates.

In order to improve the accuracy of size measurements, the nanoparticle tracking analysis of the collected supernatants was also performed, enabling the tracking of individual particles by analyzing their Brownian motion, thus providing a particle individual evaluation. NTA results (Figure 4b) evidenced the release of polyplexes with increasing size over time, from around 100 nm at 2 h of incubation up to *ca.* 150 nm at 48 h. Additionally, the concentration of the detected PXs increased over time with a significant increase between the initial time points (2 and 4 h) and the final one ($p < 0.0001$), indicating that the hydrogel released a greater quantity of polyplexes as it underwent progressive destabilization/erosion (data regarding the hydrogel erosion rate are shown in Figure S5).

The quantification of heparin-mediated siRNA release in the supernatants was also carried out by using the SYBR Gold assay. The release curve reported in Figure 4c indicates that no

https://doi.org/10.1021/acsapm.5c02686
ACS Appl. Polym. Mater. 2025, 7, 15856−15866

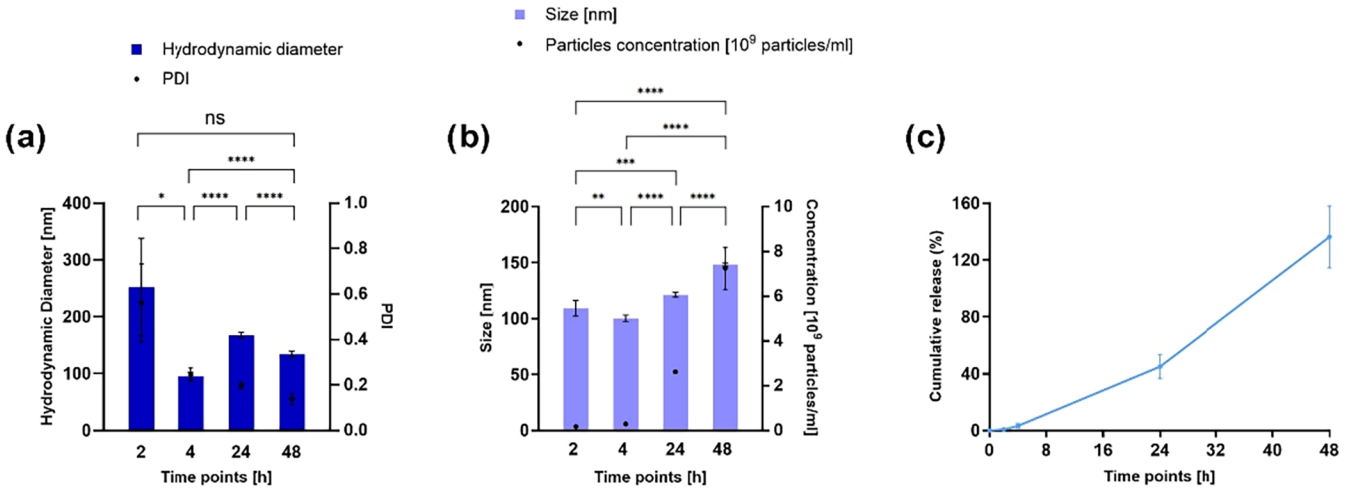

Figure 4. DLS and NTA measurements of released particles from CHP407 1.4% + α-CD 10% + PX gels. (a) DLS measurements of the supernatants collected at different time points during gel incubation in contact with PBS. Hydrodynamic diameter (left y-axis) and PDI (right y-axis) of samples collected at different time points (i.e., 2, 4, 24, and 48 h). (b) NTA measurements of the supernatants collected at different time points during gel incubation in contact with PBS. For analysis, the samples were diluted 1:100 in HEPES buffer. Size (left y-axis) and particles concentration (right y-axis) of samples collected at different time points (2, 4, 24, and 48 h). (c) Polyplexes cumulative release (%) estimated through the SYBR Gold assay (2, 4, 24, and 48 h). Data points indicate mean ± SD, n = 3. The statistical analysis reported on the graph referred exclusively to the hydrodynamic diameter and size values.

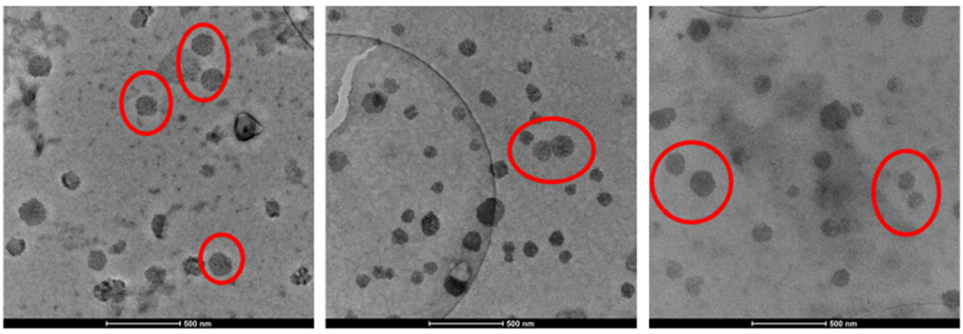

Figure 5. TEM images of the released particulate from the hydrogel. TEM imaging was performed on the released medium collected after CHP407 1.4% + CD 10% + PX gels incubation in contact with DPBS for 48 h. Intact polyplexes can be observed (red circles), surrounded by other erosion debris from the hydrogel. Scale bar = 500 nm.

burst release of siRNA occurred in the short term (release of 3% at 4 h of incubation), while complete release was achieved after 48 h of incubation, with half of the siRNA content delivered after 24 h. The achievement of a percentage of release higher than 100% at 48 h of observation can be correlated to potential interaction of the SYBR Gold assay with the polymer debris present in the supernatant.

Overall, at 48 h of incubation, corresponding to the complete release of the payload due to gel dissolution/erosion, a total siRNA content of 0.107 nmol/mL was delivered.

Lastly, to provide further evidence of the release of intact PXs from the SM hydrogel, TEM imaging was employed. In Figure 5, distinct spherical particles are clearly visible, although some background noise is also evident in the images, most likely due to other debris originating from the dissolution and erosion of the SM hydrogel. In particular, the polyplexes can be differentiated from debris by their more uniform shape, well-defined edges, and a brighter color, whereas the debris exhibited heterogeneity and appeared darker in comparison. Additionally, the dimensions and size distribution of these particles align with the measurements obtained through DLS analysis of the collected released media.

3.3. *In Vitro* Testing. *3.3.1. Polyplex Cellular Uptake.* The internalization of polyplexes by cells was assessed through an uptake experiment performed in the MHS cell line, which is a murine alveolar macrophage line with phagocytic activity, widely employed in experiments regarding inflammatory response due to their ability to produce cytokines. The measurement was carried out by flow cytometry. Cells were treated with polyplexes freshly prepared both in HEPES buffer and in α-CD (14% w/v) containing HEPES solution (PX_HEPES and PX_HEPES + α-CD, respectively) and polyplexes released from the CHP407 1.4% + α-CD 10% + PX hydrogel after 24 and 48 h of incubation (RELEASED_PX_24h and RELEASED_PX_48h, respectively). The results presented in Figure 6 provided evidence of a positive uptake of both the freshly prepared and released polyplexes from CHP407 1.4% + α-CD 10% + PX gels. In particular, the median fluorescent intensity (MFI) of the freshly prepared polyplexes was considerably higher than that of Lipofectamine (LF, positive control). This discrepancy can be attributed to the fact that Lipofectamine-based complexes may be taken up by different pathways depending on the specific cell line under investigation. This variability is influenced by factors such as

https://doi.org/10.1021/acsapm.5c02686
ACS Appl. Polym. Mater. 2025, 7, 15856−15866

the cell membrane composition, endocytic pathways, and intracellular trafficking mechanisms inherent to each cell type.[44] In addition, the MFI of the cells treated with PX_HEPES+ α-CD was significantly lower ($p < 0.0001$) compared to the cells treated with PX_HEPES, but still significantly higher than LF ($p < 0.0001$). This result can be explained considering the already reported cytotoxicity of α-CDs (Figure S6) that could have affected the activity of the cells.[36,45] Regarding the uptake of the released polyplexes, the MFI of the cells treated with polyplexes released after 24 and 48 h were lower than the positive control but still considered acceptable, as their MFI can be considered in the range of the positive control LF (no significant differences).

3.3.2. Polyplex-Mediated Gene Modulation. The capacity of the polyplexes to silence gene expression was evaluated using a qPCR experiment conducted with the THP-1 cell line, which are human not differentiated monocytes. The selection of this cell line was based on its phagocytic capabilities, similar to those of the previously utilized macrophages. Cells were treated with polyplexes (N/P 10) freshly prepared both in HEPES buffer and in α-CD (14% w/v) containing HEPES solution (PX_HEPES and PX_HEPES + α-CD, respectively) and polyplexes released from the hydrogel after 24 and 48 h of incubation (RELEASED_PX_24h and RELEASED_PX_48h, respectively). Lipofectamine 2000 lipoplexes (LF) and untreated cells were used as positive and negative control, respectively. The obtained results are summarized in Figure 7, which reports the mRNA levels measured for each tested condition. Cells treated with PX_HEPES showed downregulation in GADPH mRNA levels, aligning with expectations. Conversely, cells treated with PX_HEPES + α-CD exhibited an upregulation of GADPH gene expression. These unusual values can be explained considering the significant toxicity exerted by cyclodextrins themselves.[45,46] This toxicity may have triggered gene upregulation and consequent cell apoptosis, which can skew normalized results. A particularly promising result emerged from the polyplexes released from the hydrogel. These polyplexes exhibited an elevated capability of downregulating gene expression compared to the freshly prepared ones, and this effect was even more pronounced after 48 h (RELEASED_PX_48h). This observation clearly evidenced that the concentration of polyplexes in the release medium progressively increased over time. Eventually, the observed downregulation of GADPH gene expression in cells treated with RELEASED_PX_48h was found to be comparable to the performance of Lipofectamine lipoplexes (no significant difference), thereby confirming a promising result of the system.

4. CONCLUSION

The research conducted in this work displayed promising prospects for upcoming investigations regarding the design of injectable hydrogels for local siRNA therapy. The core of this system was a supramolecular hydrogel based on a tailored-made poly(ether urethane) and α-cyclodextrins. This hydrogel hosted PBAE-based polyplexes. Rheological tests demonstrated that the PX-loaded SM hydrogel retained its typical thixotropic and self-healing properties that are essential to ensure an easy application through injection. Upon confirming the successful encapsulation and subsequent release of the nanoparticulate systems from the hydrogels, their effectiveness was evaluated through *in vitro* experiments. A macrophage cell line was selected because of its phagocytic properties enabling PX

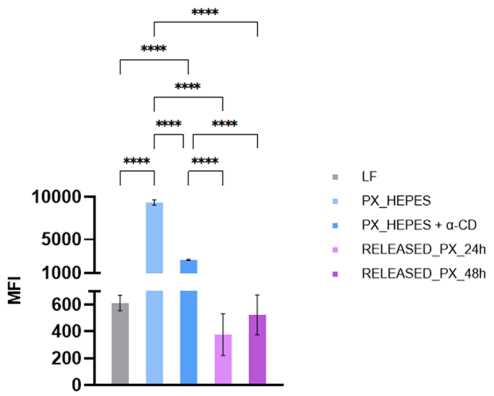

Figure 6. Polyplexes cellular uptake. MHS uptake of polyplexes quantified by flow cytometry as median fluorescence intensity (MFI) after treatment with polyplexes freshly prepared in HEPES buffer (PX_HEPES, light blue) and in α-CD (14% w/v) containing HEPES solution (PX_HEPES + α-CD, blue) and released from the gel after 24 h (RELEASED_PX_24h, light purple) and 48 h (RELEASED_PX_24h, purple) of incubation, and Lipofectamine 2000 lipoplexes (LF, gray). Data points indicate mean ± SD, $n = 3$.

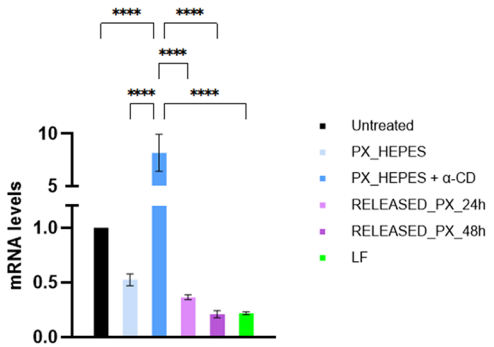

Figure 7. Polyplexes gene modulation. Measured mRNA levels after THP-1 cell treatment with polyplexes freshly prepared in HEPES buffer (PX_HEPES, light blue), polyplexes freshly prepared in α-CD (14% w/v) containing HEPES solution (PX_HEPES + α-CD, blue), polyplexes released from the gel after 24 and 48 h of incubation in contact with the release medium (RELEASED_PX_24h and RELEASED_PX_48h, purple), and Lipofectamine 2000 lipoplexes (LF, green). Untreated cells were used as a negative control (untreated, black). Data points indicate the mean ± SD of technical triplicates.

internalization and its occurrence in inflamed milieus such as arthritis, which could represent a potential application of the developed injectable formulation. With the loaded concentration of polyplexes within the hydrogel, successful cellular uptake and gene downregulation were achieved.

This study is preliminary and requires further investigation to delve deeper into the topic. For instance, a more consistent release protocol should be developed to better replicate real *in vivo* conditions. This would assist in creating a system with a sustained release profile over time. Regarding *in vitro* studies, the potential of harnessing a more biomimetic release mechanism, facilitating direct hydrogel interaction with *in vitro* cultures, emerges as a pivotal avenue for deepening our understanding of these localized drug release systems. For instance, a step forward could be achieved by designing a dynamic culture system in which cells are separated from the hydrogel by a porous membrane that allows nanocarrier progressive diffusion and direct interaction with cells.

https://doi.org/10.1021/acsapm.5c02686
ACS Appl. Polym. Mater. 2025, 7, 15856−15866

Nevertheless, given the encouraging outcomes, this study bears substantial potential for future research in the treatment of diverse pathological conditions, such as cancer, bacterial infections, neurodegenerative disorders, skin wounds, and inflammatory diseases.

■ ASSOCIATED CONTENT

Supporting Information

The Supporting Information is available free of charge at https://pubs.acs.org/doi/10.1021/acsapm.5c02686.

Chemical structures of polymers (Figures S1 and S2), preparation scheme of supramolecular hydrogel loaded with polyplexes (Figure S3), gelation process (Figure S4), hydrogel swelling and stability study (Figure S5), and cytotoxicity test (Figure S6) (PDF)

■ AUTHOR INFORMATION

Corresponding Authors

Monica Boffito − *Department of Mechanical and Aerospace Engineering, Politecnico di Torino, 10129 Torino, Italy; Istituto per i Processi Chimico Fisici (IPCF) − Centro Nazionale delle Ricerche (CNR), 56124 Pisa, Italy;* orcid.org/0000-0001-7637-2001; Email: monica.boffito@polito.it

Gianluca Ciardelli − *Department of Mechanical and Aerospace Engineering, Politecnico di Torino, 10129 Torino, Italy; Istituto per i Processi Chimico Fisici (IPCF) − Centro Nazionale delle Ricerche (CNR), 56124 Pisa, Italy;* orcid.org/0000-0003-0199-1427; Email: gianluca.ciardelli@polito.it

Olivia M. Merkel − *Department of Pharmacy, Ludwig-Maximilians-Universität München, 81377 Munich, Germany; Center for NanoScience (CeNS), Ludwig-Maximilians-Universität München, 80799 Munich, Germany;* orcid.org/0000-0002-4151-3916; Email: olivia.merkel@lmu.de

Authors

Paola Grillo Coppola − *Department of Mechanical and Aerospace Engineering, Politecnico di Torino, 10129 Torino, Italy; Department of Surgical Sciences, Università degli Studi di Torino, 10126 Torino, Italy*

Adrian Philipp Eckart Kromer − *Department of Pharmacy, Ludwig-Maximilians-Universität München, 81377 Munich, Germany*

Benjamin Winkeljann − *Department of Pharmacy, Ludwig-Maximilians-Universität München, 81377 Munich, Germany; Center for NanoScience (CeNS), Ludwig-Maximilians-Universität München, 80799 Munich, Germany;* orcid.org/0000-0002-6334-6696

Complete contact information is available at: https://pubs.acs.org/10.1021/acsapm.5c02686

Author Contributions

#P.G.C. and A.P.E.K. contributed equally to this work.

Notes

The authors declare no competing financial interest.

■ REFERENCES

(1) Yavvari, P. S.; Pal, S.; Kumar, S.; Kar, A.; Awasthi, A. K.; Naaz, A.; Srivastava, A.; Bajaj, A. Injectable, Self-Healing Chimeric Catechol-Fe(III) Hydrogel for Localized Combination Cancer Therapy. *ACS Biomater. Sci. Eng.* **2017**, *3* (12), 3404−3413.

(2) Zhang, L.; Wang, L.; Guo, B.; Ma, P. X. Cytocompatible Injectable Carboxymethyl Chitosan/N-Isopropylacrylamide Hydrogels for Localized Drug Delivery. *Carbohydr. Polym.* **2014**, *103* (1), 110−118.

(3) Overstreet, D. J.; Dutta, D.; Stabenfeldt, S. E.; Vernon, B. L. Injectable Hydrogels. *J. Polym. Sci., Part B: Polym. Phys.* **2012**, *50*, 881−903.

(4) Nguyen, K.; Dang, P. N.; Alsberg, E. Functionalized, Biodegradable Hydrogels for Control over Sustained and Localized SiRNA Delivery to Incorporated and Surrounding Cells. *Acta Biomater.* **2013**, *9* (1), 4487−4495.

(5) Han, H. D.; Mora, E. M.; Roh, J. W.; Nishimura, M.; Lee, S. J.; Stone, R. L.; Bar-Eli, M.; Lopez-Berestein, G.; Sood, A. K. Chitosan Hydrogel for Localized Gene Silencing. *Cancer Biol. Ther.* **2011**, *11* (9), 839−845.

(6) Nguyen, M. K.; Jeon, O.; Krebs, M. D.; Schapira, D.; Alsberg, E. Sustained Localized Presentation of RNA Interfering Molecules from in Situ Forming Hydrogels to Guide Stem Cell Osteogenic Differentiation. *Biomaterials* **2014**, *35* (24), 6278−6286.

(7) Segovia, N.; Pont, M.; Oliva, N.; Ramos, V.; Borrós, S.; Artzi, N. Hydrogel Doped with Nanoparticles for Local Sustained Release of SiRNA in Breast Cancer. *Adv. Healthcare Mater.* **2015**, *4* (2), 271−280.

(8) Knipe, J. M.; Strong, L. E.; Peppas, N. A. Enzyme- and PH-Responsive Microencapsulated Nanogels for Oral Delivery of SiRNA to Induce TNF-α Knockdown in the Intestine. *Biomacromolecules* **2016**, *17* (3), 788−797.

(9) Su, F. Y.; Mac, Q. D.; Sivakumar, A.; Kwong, G. A. Interfacing Biomaterials with Synthetic T Cell Immunity. *Adv. Healthcare Mater.* **2021**, *10*, No. 2100157.

(10) Harris, E.; Zimmerman, D.; Warga, E.; Bamezai, A.; Elmer, J. Nonviral Gene Delivery to T Cells with Lipofectamine LTX. *Biotechnol. Bioeng.* **2021**, *118* (4), 1693−1706.

(11) Khawar, M. B.; Afzal, A.; Si, Y.; Sun, H. Steering the Course of CAR T Cell Therapy with Lipid Nanoparticles. *J. Nanobiotechnol.* **2024**, *22*, 380.

(12) Kandil, R.; Xie, Y.; Heermann, R.; Isert, L.; Jung, K.; Mehta, A.; Merkel, O. M. Coming in and Finding Out: Blending Receptor-Targeted Delivery and Efficient Endosomal Escape in a Novel Bio-Responsive SiRNA Delivery System for Gene Knockdown in Pulmonary T Cells. *Adv. Ther.* **2019**, *2* (7), No. 1900047.

(13) Shi, J.; Huang, M. W.; Lu, Z. D.; Du, X. J.; Shen, S.; Xu, C. F.; Wang, J. Delivery of MRNA for Regulating Functions of Immune Cells. *J. Controlled Release* **2022**, *345*, 494−511.

(14) Mccaffrey, A. P.; Meuse, L.; Pham, T. T. T.; Conklin, D. S.; Hannon, G. J.; Kay, M. A. RNA interference in adult mice. *Nature* **2002**, *418* (6893), 38−39.

(15) Davis, M. E.; Zuckerman, J. E.; Choi, C. H. J.; Seligson, D.; Tolcher, A.; Alabi, C. A.; Yen, Y.; Heidel, J. D.; Ribas, A. Evidence of RNAi in Humans from Systemically Administered SiRNA via Targeted Nanoparticles. *Nature* **2010**, *464* (7291), 1067−1070.

(16) Mali, S. Delivery Systems for Gene Therapy. *Indian J. Hum. Genet.* **2013**, *19*, 3−8.

(17) Sainz-Ramos, M.; Gallego, I.; Villate-Beitia, I.; Zarate, J.; Maldonado, I.; Puras, G.; Pedraz, J. L. How Far Are Non-viral Vectors to Come of Age and Reach Clinical Translation in Gene Therapy? *Int. J. Mol. Sci.* **2021**, *22* (14), No. 7545.

(18) Patil, Y.; Panyam, J. Polymeric Nanoparticles for SiRNA Delivery and Gene Silencing. *Int. J. Pharm.* **2009**, *367* (1−2), 195−203.

(19) Piotrowski-Daspit, A. S.; Kauffman, A. C.; Bracaglia, L. G.; Saltzman, W. M. Polymeric Vehicles for Nucleic Acid Delivery. *Adv. Drug Delivery Rev.* **2020**, *156*, 119−132.

(20) Wang, H.; Zhang, S.; Lv, J.; Cheng, Y. Design of Polymers for SiRNA Delivery: Recent Progress and Challenges. *VIEW* **2021**, *2* (3), No. 20200026.

(21) Paunovska, K.; Loughrey, D.; Dahlman, J. E. Drug Delivery Systems for RNA Therapeutics. *Nature Rev. Genet.* **2022**, *23*, 265−280.
(22) Cordeiro, R. A.; Serra, A.; Coelho, J. F. J.; Faneca, H. Poly(β-Amino Ester)-Based Gene Delivery Systems: From Discovery to Therapeutic Applications. *J. Controlled Release* **2019**, *310*, 155−187.
(23) Kozielski, K. L.; Tzeng, S. Y.; Green, J. J. A Bioreducible Linear Poly(β-Amino Ester) for SiRNA Delivery. *Chem. Commun.* **2013**, *49* (46), 5319−5321.
(24) Kozielski, K. L.; Ruiz-Valls, A.; Tzeng, S. Y.; Guerrero-Cázares, H.; Rui, Y.; Li, Y.; Vaughan, H. J.; Gionet-Gonzales, M.; Vantucci, C.; Kim, J.; Schiapparelli, P.; Al-Kharboosh, R.; Quiñones-Hinojosa, A.; Green, J. J. Cancer-Selective Nanoparticles for Combinatorial SiRNA Delivery to Primary Human GBM in Vitro and in Vivo. *Biomaterials* **2019**, *209*, 79−87.
(25) Merkel, O. M. Can Pulmonary RNA Delivery Improve Our Pandemic Preparedness? *J. Controlled Release* **2022**, *345*, 549−556.
(26) Dosta, P.; Ramos, V.; Borrós, S. Stable and Efficient Generation of Poly(β-Amino Ester)s for RNAi Delivery. *Mol. Syst. Des. Eng.* **2018**, *3* (4), 677−689.
(27) Vetter, V. C.; Wagner, E. Targeting Nucleic Acid-Based Therapeutics to Tumors: Challenges and Strategies for Polyplexes. *J. Controlled Release* **2022**, *346*, 110−135.
(28) Jin, Y.; Wang, X.; Kromer, A. P. E.; Müller, J. T.; Zimmermann, C.; Xu, Z.; Hartschuh, A.; Adams, F.; Merkel, O. M. Role of Hydrophobic Modification in Spermine-Based Poly(β-Amino Ester)s for SiRNA Delivery and Their Spray-Dried Powders for Inhalation and Improved Storage. *Biomacromolecules* **2024**, *25*, 4177−4191.
(29) Steinegger, K. M.; Allmendinger, L.; Sturm, S.; Sieber-Schäfer, F.; Kromer, A. P. E.; Müller-Caspary, K.; Winkeljann, B.; Merkel, O. M. Molecular Dynamics Simulations Elucidate the Molecular Organization of Poly(Beta-Amino Ester) Based Polyplexes for SiRNA Delivery. *Nano Lett.* **2024**, *24* (49), 15683−15692.
(30) Li, J.; Ni, X.; Leong, K. W. Injectable Drug-Delivery Systems Based on Supramolecular Hydrogels Formed by Poly(Ethylene Oxide)s and-Cyclodextrin. *J. Biomed. Mater. Res., Part A* **2003**, *65A* (2), 196−202.
(31) Pradal, C.; Jack, K. S.; Grøndahl, L.; Cooper-White, J. J. Gelation Kinetics and Viscoelastic Properties of Pluronic and α-Cyclodextrin-Based Pseudopolyrotaxane Hydrogels. *Biomacromolecules* **2013**, *14* (10), 3780−3792.
(32) Li, J.; Loh, X. J. Cyclodextrin-Based Supramolecular Architectures: Syntheses, Structures, and Applications for Drug and Gene Delivery. *Adv. Drug Delivery Rev.* **2008**, *60* (9), 1000−1017.
(33) Giuliano, E.; Paolino, D.; Fresta, M.; Cosco, D. Mucosal Applications of Poloxamer 407-Based Hydrogels: An Overview. *Pharmaceutics* **2018**, *10* (3), No. 159.
(34) Torchio, A.; Boffito, M.; Gallina, A.; Lavella, M.; Cassino, C.; Ciardelli, G. Supramolecular Hydrogels Based on Custom-Made Poly(Ether Urethane)s and Cyclodextrins as Potential Drug Delivery Vehicles: Design and Characterization. *J. Mater. Chem. B* **2020**, *8* (34), 7696−7712.
(35) Torchio, A.; Cassino, C.; Lavella, M.; Gallina, A.; Stefani, A.; Boffito, M.; Ciardelli, G. Injectable Supramolecular Hydrogels Based on Custom-Made Poly(Ether Urethane)s and α-Cyclodextrins as Efficient Delivery Vehicles of Curcumin. *Mater. Sci. Eng., C* **2021**, *127*, No. 112194.
(36) Torchio, A.; Boffito, M.; Laurano, R.; Cassino, C.; Lavella, M.; Ciardelli, G. Double-Crosslinkable Poly(Urethane)-Based Hydrogels Relying on Supramolecular Interactions and Light-Initiated Polymerization: Promising Tools for Advanced Applications in Drug Delivery. *J. Mater. Chem. B* **2024**, *12* (34), 8389−8407.
(37) Crivello, G.; Orlandini, G.; Morena, A. G.; Torchio, A.; Mattu, C.; Boffito, M.; Tzanov, T.; Ciardelli, G. Lignin−Cobalt Nano-Enabled Poly(Pseudo)Rotaxane Supramolecular Hydrogel for Treating Chronic Wounds. *Pharmaceutics* **2023**, *15* (6), No. 1717.
(38) Carneiro, S. P.; Müller, J. T.; Merkel, O. M. Fluorescent Techniques for RNA Detection in Nanoparticles. In *RNA Amplification and Analysis*; Astatke, M., Ed.; Methods in Molecular Biology; Humana: New York, NY, 2024; Vol. *2822*, pp 187−203 DOI: 10.1007/978-1-0716-3918-4_14.
(39) Loftsson, T.; Sigurdsson, H. H.; Jansook, P. Anomalous Properties of Cyclodextrins and Their Complexes in Aqueous Solutions. *Materials* **2023**, *16* (6), No. 2223.
(40) He, C.; Hu, Y.; Yin, L.; Tang, C.; Yin, C. Effects of Particle Size and Surface Charge on Cellular Uptake and Biodistribution of Polymeric Nanoparticles. *Biomaterials* **2010**, *31* (13), 3657−3666.
(41) Jin, Y.; Adams, F.; Nguyen, A.; Sturm, S.; Carnerio, S.; Müller-Caspary, K.; Merkel, O. M. Synthesis and Application of Spermine-Based Amphiphilic Poly(β-Amino Ester)s for SiRNA Delivery. *Nanoscale Adv.* **2023**, *5* (19), 5256−5262.
(42) Revdekar, A.; Salvi, B. V.; Shende, P. Active Transfection of Genetic Materials Using Cyclodextrin-Anchored Nanovectors. *Mater. Adv.* **2024**, *5*, 9548−9564.
(43) Xing, Y.; Meng, B.; Chen, Q. Cyclodextrin-Containing Drug Delivery Systems and Their Applications in Neurodegenerative Disorders. *Int. J. Mol. Sci.* **2024**, *25* (19), No. 10834.
(44) Cardarelli, F.; Digiacomo, L.; Marchini, C.; Amici, A.; Salomone, F.; Fiume, G.; Rossetta, A.; Gratton, E.; Pozzi, D.; Caracciolo, G. The Intracellular Trafficking Mechanism of Lipofectamine-Based Transfection Reagents and Its Implication for Gene Delivery. *Sci. Rep.* **2016**, *6*, No. 25879.
(45) Róka, E.; Ujhelyi, Z.; Deli, M.; Bocsik, A.; Fenyvesi, É.; Szente, L.; Fenyvesi, F.; Vecsernyés, M.; Váradi, J.; Fehér, P.; Gesztelyi, R.; Félix, C.; Perret, F.; Bácskay, I. K. Evaluation of the Cytotoxicity of α-Cyclodextrin Derivatives on the Caco-2 Cell Line and Human Erythrocytes. *Molecules* **2015**, *20* (11), 20269−20285.
(46) Bernal, L.; Alvarado-Vázquez, A.; Ferreira, D. W.; Paige, C. A.; Ulecia-Morón, C.; Hill, B.; Caesar, M.; Romero-Sandoval, E. A. Evaluation of a Nanotechnology-Based Approach to Induce Gene-Expression in Human THP-1 Macrophages under Inflammatory Conditions. *Immunobiology* **2017**, *222* (2), 399−408.